International Journal of Mass Spectrometry 280 (2009) 6–11

Contents lists available at ScienceDirect

International Journal of Mass Spectrometry

journal homepage: www.elsevier.com/locate/ijms

Reactions of small negative ions with $O_2(a\ ^1\Delta_g)$ and $O_2(X\ ^3\Sigma_g^-)$

Anthony Midey[a,b], Itzhak Dotan[a,c], J.V. Seeley[d], A.A. Viggiano[a,*]

[a] Air Force Research Laboratory, Space Vehicles Directorate, 29 Randolph Road, Hanscom Air Force Base, MA 01731-3010, United States
[b] Under Contract to the Institute for Scientific Research, Boston College, Chestnut Hill, MA 02467, United States
[c] The Open University of Israel, 108 Ravutski Street, Raanana 43107, Israel
[d] Department of Chemistry, Oakland University, Rochester, MI 48309-4401, United States

ARTICLE INFO

Article history:
Received 27 March 2008
Received in revised form 2 May 2008
Accepted 8 May 2008
Available online 16 May 2008

Keywords:
Negative ions
Penning detachment
Rate constants
Excited oxygen

ABSTRACT

The rate constants and product ion branching ratios were measured for the reactions of various small negative ions with $O_2(X\ ^3\Sigma_g^-)$ and $O_2(a\ ^1\Delta_g)$ in a selected ion flow tube (SIFT). Only NH_2^- and CH_3O^- were found to react with $O_2(X)$ and both reactions were slow. CH_3O^- reacted by hydride transfer, both with and without electron detachment. NH_2^- formed both OH^-, as observed previously, and O_2^-, the latter via endothermic charge transfer. A temperature study revealed a negative temperature dependence for the former channel and Arrhenius behavior for the endothermic channel, resulting in an overall rate constant with a minimum at 500 K. SF_6^-, SF_4^-, SO_3^- and CO_3^- were found to react with $O_2(a\ ^1\Delta_g)$ with rate constants less than 10^{-11} cm^3 s^{-1}. NH_2^- reacted rapidly with $O_2(a\ ^1\Delta_g)$ by charge transfer. The reactions of HO_2^- and SO_2^- proceeded moderately with competition between Penning detachment and charge transfer. SO_2^- produced a SO_4^- cluster product in 2% of reactions and HO_2^- produced O_3^- in 13% of the reactions. CH_3O^- proceeded essentially at the collision rate by hydride transfer, again both with and without electron detachment. These results show that charge transfer to $O_2(a\ ^1\Delta_g)$ occurs readily if the there are no restrictions on the ion beyond the reaction thermodynamics. The SO_2^- and HO_2^- reactions with $O_2(a)$ are the only known reactions involving Penning detachment besides the reaction with O_2^- studied previously [R.S. Berry, Phys. Chem. Chem. Phys., 7 (2005) 289–290].

Published by Elsevier B.V.

1. Introduction

We have recently developed a technique to study the kinetics of the ion chemistry of $O_2(a\ ^1\Delta_g)$ more accurately than has been done in the past [2,3]. The method relies on a calibrated emission cell to determine absolute $O_2(a\ ^1\Delta_g)$ flow rates. Recent advances in thermoelectrically cooled InGaAs photodiodes have enabled the method for use with flow tube instruments. $O_2(a\ ^1\Delta_g)$ is detected with good sensitivity by observing its emission intensity in the strongly forbidden $(a\ ^1\Delta_g,\ v'=0) \rightarrow (X\ ^3\sum_g^-,\ v''=0)$ band at 1270 nm [4].

We have used two methods to generate $O_2(a\ ^1\Delta_g)$. In the first study [2], a microwave discharge on a mixture of O_2 in He produced not only $O_2(a\ ^1\Delta_g)$, but also O, $O_2(X,\ v''=0)$, and O_3. Since these species are quite reactive [5–7], the chemistry involving these species must be known in order to determine accurate kinetics for $O_2(a\ ^1\Delta_g)$. These species could not be completely quenched, which is especially problematic with respect to O and $O_2(X,\ v>0)$ reactions because accurate measurements of the rate constants for these contaminants are difficult. Unless the $O_2(a\ ^1\Delta_g)$ rate constant is comparable to or larger than those for the other oxygen species, the experimental value will have large uncertainties after correcting for the trace impurities. For that reason, we have also developed a chemical-based method for generating $O_2(a\ ^1\Delta_g)$ [3].

Most previous studies of the ion chemistry of $O_2(a\ ^1\Delta_g)$ have concentrated on the key ionospheric reactions that convert ions into electrons [2,3,8,9] namely

$$O_2^- + O_2(a^1\Delta_g) \rightarrow 2O_2 + e + 51.5\,\text{kJ mol}^{-1} \quad (1)$$

and

$$O^- + O_2(a^1\Delta_g) \rightarrow O_3 + e + 60.3\,\text{kJ mol}^{-1} \quad (2a)$$

$$\rightarrow O_2^- + O - 3.0\,\text{kJ mol}^{-1}. \quad (2b)$$

The thermochemistry above has been calculated from the NIST Webbook values [10]. A major motivation for the development of our technique was to help settle a controversy on the correct rate constant for both reactions (1) and (2). Previously reported rate constants differ by about an order of magnitude [8,9]. Our recent studies in a selected ion flow tube (SIFT) have shown that the previous measurements at 298 K for both reactions have considerable

* Corresponding author. Tel.: +1 781 377 4028; fax: +1 781 377 1148.
E-mail addresses: afrl.rvb.pa@hanscom.af.mil, Albert.Viggiano@hanscom.af.mil (A.A. Viggiano).

1387-3806/$ – see front matter. Published by Elsevier B.V.
doi:10.1016/j.ijms.2008.05.010

uncertainties. We have also observed product channel 2b for the first time [2,3]. The temperature dependences have also been measured from 200 to 700 K. The rate constant for reaction (1) is found to be collisional at all temperatures, while reaction (2a) has a rate constant that is essentially constant and slow at all temperatures. Reaction (2b) has a rate constant that increases with increasing temperature as expected for an endothermic reaction that becomes energetically allowed at higher temperatures [3].

Other than these two reactions, few studies of the ion chemistry involving $O_2(a\ ^1\Delta_g)$ have been performed. A rough estimate for the rate constant for vibrational quenching of $NO^+(X,\ v > 0)$ by $O_2(a\ ^1\Delta_g)$ has been made by Dotan et al. [11] The reaction of SO_2^- with $O_2(a\ ^1\Delta_g)$ has been studied qualitatively in a flowing afterglow by Grabowski et al. to bracket the electron affinity (EA) of SO_2 [12]. Bierbaum and co-workers have also studied the products generated in the reactions of carbanions with $O_2(X)$ and $O_2(a)$ in a flowing afterglow [13,14]. In all of those experiments, the $O_2(a)$ concentration was not known quantitatively.

The goal of this study is to expand the database of kinetics involving $O_2(a\ ^1\Delta_g)$ reactions with negative ions. However, as a mixture of $O_2(a)$ and $O_2(X)$ in He is produced by the chemical singlet oxygen generator, the first step has been to determine if the chosen ions react with $O_2(X\ ^3\Sigma_g^-)$. If this chemistry is unknown, measurements of the rate constants and product ion branching ratios with pure O_2 have been made. We have currently focused on anions with relatively few atoms. In particular, we have emphasized ions that are found to make important contributions to ionospheric chemistry or that could utilize the ~1 eV of electronic energy available in $O_2(a\ ^1\Delta_g)$ to drive an endothermic process such as that observed in the charge transfer reaction (2b). In the process, some new examples of Penning detachment of an electron from a negative ion through reaction with an excited neutral have been found [1].

2. Experimental

The measurements were made in the SIFT at the Air Force Research Laboratory. This technique for measuring ion–molecule kinetics was described in detail previously [2,15] and only a brief description of the method is given here, except for a discussion of the chemical generation of $O_2(a\ ^1\Delta_g)$. Briefly, ions were created in an external ion source chamber via electron impact on an appropriate source gas (see below). The ion of interest was then mass selected with a quadrupole mass filter and injected into a flow tube through a Venturi inlet. A helium buffer (AGA, 99.995%) carried the ions downstream where $O_2(a\ ^1\Delta_g)$ was added through a Pyrex inlet 49 cm upstream from a sampling nose cone aperture. The primary ions and product ions were monitored by a quadrupole mass analyzer and detected with a particle multiplier. Kinetics were measured by monitoring the decay of the reactant ion signal as a function of $O_2(a\ ^1\Delta_g)$ concentration added.

Here we used a chemical generator for producing $O_2(a\ ^1\Delta_g)$, which is shown in Fig. 1 along with the detection system. Chlorine (Aldrich 99.5+%) was bubbled through a basic solution of hydrogen peroxide and converted into O_2 as shown in the following equation:

$$H_2O_2 + Cl_2 + 2KOH \rightarrow O_2 + 2KCl + 2H_2O. \quad (3)$$

This reaction is well known to produce both ground electronic state $O_2(X\ ^3\Sigma_g^-)$ and $O_2(a\ ^1\Delta_g)$ [16,17] and was used as a source of $O_2(a\ ^1\Delta_g)$ to create a chemical O_2/I_2 laser (COIL) [18]. In that application, the reaction used 90% hydrogen peroxide at atmospheric pressure, typically giving an $O_2(a\ ^1\Delta_g)$ yield of 30–40%. In our case, the pressure was low (3–8 Torr) and 35% (w/w) H_2O_2 (Alfa Aesar) was used, resulting in smaller conversion yields.

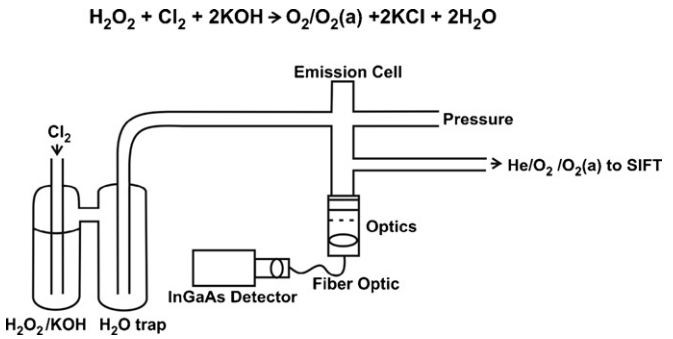

Fig. 1. Schematic diagram of the chemical singlet oxygen generator with emission detection adapted for the selected ion flow tube (SIFT).

The basic H_2O_2 solution was a mixture of 60 ml of 35% (w/w) H_2O_2 and 40 ml of 4.04 M KOH. The solutions were mixed very slowly at 0 °C because the heat of solution was large and the cold bath prevented thermal decomposition of H_2O_2 during the mixing. The solution was then attached to the first bubbler on the SIFT and immersed in a methanol bath held at −16 °C by a recirculating chiller. The solution was then pumped on with a mechanical pump to remove trapped gases.

Keeping the mixture at low temperature created a slushy mixture inside the reactor and accomplished three things. First, lowering the temperature of the solution prevented decomposition of the hydrogen peroxide during reaction (3), which is highly exothermic. Second, the vapor pressure of the aqueous solution was lowered. Third, we found that the highest yields of $O_2(a\ ^1\Delta_g)$ occurred at the lower bath temperatures, possibly because the amount of gas phase water was reduced. Even lower temperatures were not possible because the solution froze completely, resulting in transient and unreliable, i.e., short lived, production of $O_2(a\ ^1\Delta_g)$.

Two gas flows were added to the slushy KOH/H_2O_2 reaction mixture through a 12-mm Pyrex gas dispersion tube with a horizontal disk comprised of a coarse glass frit (Chemglass) at the bottom. A fixed flow of 15 sccm of He (Middlesex Gases, 99.9999%) was added first to prevent freezing on the glass frit and to create channels for the gases to escape. Then, a second variable flow of a 20% mixture of Cl_2 in He (AGA, 99.995%) was introduced. A gas mixture was used so that larger gas flows could be used, increasing the $O_2(a\ ^1\Delta_g)$ yield presumably by reducing wall quenching. The flush gas also helped with reducing the residence time. All of the Cl_2 was converted to a mixture of ground and excited electronic state O_2 and the solution products. The Cl_2 conversion was monitored using Cl^- generated in the flow tube using the known reactions of O^- and O_2^- with Cl_2 [19]. Periodic checks were necessary as the conversion became incomplete over the course of a day.

To avoid having water enter the flow tube, we used a second trap after the reactor that was kept at −70 °C with a methanol–liquid nitrogen slush bath. Water was detrimental in two ways. First, the technique for measuring the absolute $O_2(a\ ^1\Delta_g)$ concentration relied on having only He and O_2 in the downstream flow. Second, H_2O reacted with some of the reactant ions [19]. This trap had to be emptied after a few hours of operation because the temperature difference between the reaction vessel and the trap had the side effect of transferring the water from the first to the second colder trap. Eventually, the water formed an ice surface that caused the $O_2(a\ ^1\Delta_g)$ to be quenched. After the second trap, essentially only $O_2(X)$, $O_2(a)$, and He remained in the gas flow, verified by studying species that react with Cl_2 and H_2O.

The mixture of O_2 species and helium then passed through an optical emission cell to determine the amount of $O_2(a\ ^1\Delta_g)$. The details of the detection system were given in our previous

paper [2]. Briefly, we monitored the weak emission from the $O_2(a\ ^1\Delta_g \rightarrow X^3\Sigma_g)$ 0–0 transition at 1270 nm passed through a 5-nm bandwidth interference filter into a fiber optic bundle coupled to a thermo-electrically cooled InGaAs infrared detector with built-in amplifier. The output of the detector was read by an electrometer with considerable internal filtering to obtain relative $O_2(a\ ^1\Delta_g)$ concentrations, which were converted to absolute values by calibrating the detector output with an absolute $O_2(a\ ^1\Delta_g)$ spectrometer [2]. With the chemical generator, we found maximum concentrations of $O_2(a\ ^1\Delta_g)$ in the emission cell of $\sim 8 \times 10^{15}$ molecule cm^{-3}, which is ~15% of the total O_2 flow. Lower flows of Cl_2 resulted in lower conversion percentages.

Flow rates of $O_2(a\ ^1\Delta_g)$ were determined as follows. The fractional abundance of $O_2(a\ ^1\Delta_g)$ in the emission cell was simply the ratio of the $O_2(a\ ^1\Delta_g)$ concentration determined from the emission measurement to the total gas concentration in the cell determined by measuring the total pressure in the cell. Multiplying the total gas flow rate by the fractional abundance of $O_2(a\ ^1\Delta_g)$ gave the flow rate of $O_2(a)$ entering the flow tube in standard $cm^3\ min^{-1}$ (sccm). This flow rate could then be converted to the concentration of $O_2(a)$ present in the flow tube under the conditions of the buffer flow rate, temperature and pressure in the flow tube for determining the rate constant. Note that the O_2^- reacted with $O_2(a\ ^1\Delta_g)$ at the collisional value, indicating that losses after the cell were negligible. The absence of water was thus critical for accurate determinations.

Before entering the flow tube, the $O_2(a)$ gas mixture passed through a multi-turn Teflon needle valve with a 0.125-in. orifice (Cole-Parmer, EW-06393-61) that was used both to isolate the chemical generator and emission detection system from the flow tube and to increase the total pressure in the emission cell, making the $O_2(a\ ^1\Delta_g)$ measurement easier by increasing the absolute gas concentration. The possibility of quenching in the valve was ruled out by comparing the room temperature rate constants for the reaction of O_2^- with $O_2(a\ ^1\Delta_g)$ using the chemical generator with our previous measurement using the microwave discharge generator that did not use a valve. Excellent agreement was found between the values determined using the two different generation methods. In addition, the O_2^- rate constant was found to be collisional indicating that the concentration was not reduced. The rate constant for the O_2^- reaction with $O_2(a)$ was measured frequently to ensure the reliability of the system.

For the ions where the reactivity with $O_2(X)$ was not known, the rate constants and product ion branching ratios were measured using pure O_2 (Massachusetts Oxygen, 99.999%). The concentrations of stable reactant neutrals could be accurately measured. Therefore, the rate constants for the reactions with $O_2(X)$ had relative uncertainties of ±15% and absolute uncertainties of ±25%. Given the additional uncertainties in determining the concentrations of $O_2(a\ ^1\Delta_g)$ and the complexity of the experiments, the rate constants for these measurements had relative uncertainties of ±25% and absolute uncertainties of ±35% [3].

The branching ratios for reactions where electron detachment occurred were difficult to measure. The occurrence of the detachment channel was followed by monitoring the total current at the nose cone aperture. As ions were converted to electrons, the total current reaching the nose cone decreased because electrons created in the flow tube rapidly diffused to the walls. However, the observed nose cone current also reflected the loss of any product ions that also underwent detachment through secondary reactions with the O_2 in the flow tube. Thus, to find the amount of each product channel including detachment, the branching ratios were determined by first subtracting the sum of the product ion counts measured at each O_2 concentration from the counts of the reactant ion lost to the overall reaction at that concentration. The remainder of the reactant ion counts lost reflected the relative amount of the detachment process. Then, the counts determined for each product channel were normalized to the total product counts to find the branching ratio as a function of O_2 concentration. These branching ratios were plotted vs. O_2 concentration and extrapolated to zero O_2 concentration to determine the reported branching ratios. This extrapolation corrected for the secondary reaction of any of the primary product ions. The downstream quadrupole resolution was kept low to minimize mass discrimination. In light of the difficulty of the measurements, the branching ratios had uncertainties of ±15%.

3. Source materials

The following neutral reagents were used in the source to create the reactant ions as indicated: 5% SF_6 (Matheson, CP Grade) in He (AGA, 99.995%) for SF_6^- and SF_5^-; 10% SF_4 (Matheson, 90–94%) in He for SF_4^-; SO_2 (Matheson, 99.98%) for SO_2^- and SO_3^-; CO_2 (Matheson, 99.999%) for CO_3^-; CH_3OH (J.T. Baker, HPLC Grade) for CH_3O^-; 35% (w/w) H_2O_2 for HO_2^-; NH_3 (Matheson, 99.99%) for NH_2^-; N_2O_4 (Matheson, 99.5%) for NO_2^-; distilled water for OH^-.

4. Results and discussion

4.1. Reactions with $O_2(X\ ^3\Sigma_g^-)$

In order to measure $O_2(a\ ^1\Delta_g)$ kinetics, one must first understand O_2 ground electronic state kinetics because a mixture of the two states is present simultaneously in the SIFT. Thus, we have added $O_2(X)$ separately and measured the kinetics when reactivity has been found. Most of the ions studied here do not react measurably with $O_2(X)$ [6,20,21]; therefore, an upper limit of $1 \times 10^{-12}\ cm^3\ s^{-1}$ can be given for those rate constants. However, CH_3O^- and NH_2^- do react with $O_2(X)$, albeit slowly. Table 1 shows the results for these two ions at 300 K.

CH_3O^- reacts very slowly with $O_2(X)$ by mostly hydride transfer to produce HO_2^- with a total rate constant of $1.1 \times 10^{-12}\ cm^3\ s^{-1}$, which is just within the detection limit of the SIFT. Bierbaum and co-workers have studied this reaction previously in a flowing afterglow (FA) and saw no reaction [13,14]. The FA technique has no upstream mass spectrometer to select a reactant ion; rather, the ions are generated in the flow tube and the source gas will be present throughout. Thus, a few percent decline of the reactant ion signal would be difficult to distinguish given the possibility of reactions with small impurities in the FA. The SIFT method is more sensitive to such slow reactions given the mass selection of the reactant ion inherent in the technique.

In addition, there is a small reactive detachment channel with CH_3O^-, as well, that differs from the hydride transfer channel only in that the electron escapes from HO_2^-. This channel is endothermic by 21 kJ mol^{-1} at room temperature. An approximate upper limit to the rate constant for the detachment channel can be given by the product of the Langevin collision rate constant ($9 \times 10^{-9}\ cm^3\ s^{-1}$) and $e^{-\Delta H/RT}$. This approximate upper limit is $6 \times 10^{-12}\ cm^3\ s^{-1}$ is in good agreement with the measured value, indicating that the reaction is very efficient when allowed. The reaction with $O_2(X)$ is

Table 1
Rate constants and branching ratios for $O_2(X\ ^3\Sigma_g^-)$ reacting with CH_3O^- and NH_2^- at 300 K measured in the selected ion flow tube (SIFT)

Ion	Rate constant [collision rate constant] ($\times 10^{-10}\ cm^3\ s^{-1}$)	Products	ΔH_{rxn} (kJ mol^{-1})
NH_2^-	0.24 [9.0]	$OH^- + HNO$ (>0.98)	−148
		$O_2^- + NH_2$ (<0.02)	31
CH_3O^-	0.011 [7.4]	$HO_2^- + CH_2O$ (0.85)	−79
		$e^- + CH_2O + HO_2$ (0.15)	21

Heats of reactions are calculated using values in the NIST Webbook.

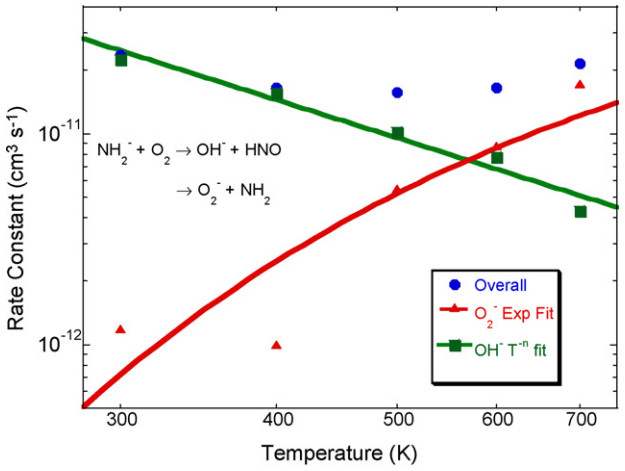

Fig. 2. Rate constants for NH_2^- with O_2. Circles, triangles and squares represent the overall rate constant, the rate constant for O_2^- production, and the rate constant for OH^- production, respectively. The O_2^- data are fit to an Arrhenius function and the OH^- data to a power law.

too slow to affect the determination of the $O_2(a\ ^1\Delta_g)$ kinetics with CH_3O^-.

NH_2^- reacts with $O_2(X)$ to form almost exclusively OH^- at 300 K. The measured rate constant is 2.4×10^{-11} cm^3 s^{-1}, which is somewhat smaller than the previous value of 4.6×10^{-11} cm^3 s^{-1} [22]. This reactivity is interesting because the strong O_2 bond is broken, which probably accounts for the slow reactivity. A small amount (<5%) of an endothermic charge transfer is also observed. As slow reactions often have interesting temperature dependences and because two product channels are formed, we have studied this reaction as a function of temperature from 300 to 700 K. Note that the CH_3O^- rate constant is just measurable in our apparatus, so a similar study is not feasible for that ion.

The overall rate constant for NH_2^- and the rate constant for each product channel are plotted in Fig. 2. Interestingly, the overall rate constant for NH_2^- at first decreases with increasing temperature, then rises at temperatures above 500 K. This trend results from the two product channels displaying completely different behavior. The exothermic OH^- channel decreases with temperature according to $T^{-1.9}$. A power law fit to that channel reproduces the data reasonably well as seen in Fig. 2. There is perhaps a hint of a steeper negative temperature dependence at higher temperature that may be due to an increasing level of vibrational excitation in NH_2^- or competition with the O_2^- channel. The branching ratio for this charge transfer product channel becomes larger than that for the OH^- channel at temperatures above 600 K. The O_2^- channel is endothermic by 31 kJ mol^{-1} and that channel increases steeply with increasing temperature as it becomes more accessible at higher energies.

A fit of the overall rate constant to the Arrhenius expression represents the data reasonably well; although, there is a fair amount of scatter around the fit, particularly at lower temperatures where the O_2^- channel is small and a larger correction must be made to account for reaction of NH_2^- with trace O_2 impurities found in the helium buffer. Approximately half of the NH_2^- was consumed in the absence of added O_2 at 300 and 400 K. The activation energy of 21 kJ mol^{-1} using the 400 K and higher data only is slightly smaller than the endothermicity, which may reflect a competition between the two channels or the influence of NH_2^- vibrational excitation.

4.2. Reactions with $O_2(a\ ^1\Delta_g)$

Table 2 shows the kinetics for reactions of various negative ions with $O_2(a\ ^1\Delta_g)$ at 300 K. SF_6^-, SF_4^-, SO_3^- and CO_3^- are unreactive, having rate constants <10^{-11} cm^3 s^{-1}, which are the smallest rate constants we can measure for $O_2(a\ ^1\Delta_g)$ reactions. This lack of reactivity is observed even though all four reactions have exothermic or nearly thermoneutral reaction pathways. Charge transfer is possible for both SF_6^- and SF_4^-, but it does not occur as seen previously with $O_2(X)$ [20]. As discussed below, charge transfer to $O_2(a\ ^1\Delta_g)$ does not seem to have an intrinsic barrier, so the bottleneck most probably involves SF_n^- neutralization. For SF_6^- charge transfer, this bottleneck is well known and is a reflection of the geometry differences between the neutral and the ion that cause poor Franck Condon overlap [23–25]. A previous study of charge transfer reactions with SF_4^- has found no such restrictions [21]. However, charge transfer from SF_4^- to $O_2(a\ ^1\Delta_g)$ is endothermic. The experimental value of the EA of SF_4 is 1.5 ± 0.2 eV [21], giving an endothermicity of 7 ± 20 kJ mol^{-1} for charge exchange. G3 calculations [26] yield an electron affinity of 1.64 eV, translating into an endothermicity of 20 kJ mol^{-1}. G3 calculations reproduce the EA of SF_6 very accurately and the theoretical value agrees with the experimental value within the uncertainties [27]. Upper limits to the charge transfer rate constants for SF_4^- of about 4×10^{-11} cm^3 s^{-1} and 2×10^{-13} cm^3 s^{-1} are found if the experimental and G3 electron affinities are used, respectively. The former rate constant is measurable in the SIFT, while the latter is not. Therefore, the absence of reactivity favors the G3 value if the assumption holds that no bottlenecks to reactivity are present besides energetics.

In the reaction of SO_3^- with $O_2(a\ ^1\Delta_g)$, SO_4^- production is highly exothermic, but it is not observed, similar to studies with $O_2(X)$ [20]. Presumably, the necessity of breaking the O_2 bond creates a barrier to reaction. The reaction of CO_3^- with $O_2(a)$ to form O_3^- is slightly endothermic. However, the endothermicity is small enough that the reaction would be observable at room temperature if no further barrier to reaction exists.

Of the reactive ionic species, only NH_2^- gives a single product ion. Charge transfer is driven by the electronic energy in $O_2(a\ ^1\Delta_g)$ and is 58 kJ mol^{-1} exothermic, proceeding at the Langevin collision rate within the experimental uncertainty. The possibility of OH^- production cannot be completely eliminated since >85% $O_2(X)$ is generated and that species has been shown above to generate OH^- almost exclusively at 300 K. Therefore, a small contribution of an OH^- product ion channel from the $O_2(a\ ^1\Delta_g)$ reaction with

Table 2
Rate constants and product branching ratios for $O_2(a\ ^1\Delta_g)$ reacting with a variety of negative ions

Ion	Rate constant [collisional value] ($\times 10^{-10}$ cm^3 s^{-1})	Products	ΔH_{rxn} (kJ mol^{-1})
SF_6^-	<0.1	$O_2^- + SF_6$	−38
SF_4^-	<0.1	$O_2^- + SF_4$	7[a]
			20[b]
SO_2^-	1.3 [6.4]	$O_2^- + SO_2$ (0.50)	−31
		$e^- + SO_2 + O_2$ (0.48)	7
		SO_4^- (0.02)	−429
SO_3^-	<0.1	$SO_4^- + O$	−23
CO_3^-	<0.1	$O_3^- + CO_2$	7[c]
CH_3O^-	6.9 [7.4]	$HO_2^- + CH_2O$ (0.52)	−174
		$e^- + CH_2O + HO_2$ (0.48)	−68
HO_2^-	3.2 [7.3]	$e^- + HO_2 + O_2$ (0.58)	4
		$O_2^- + HO_2$ (0.29)	−34
		$O_3^- + HO$ (0.13)	−19
NH_2^-	9.0 [9.0]	$O_2^- + NH_2$ (≥0.95)	−58
		$OH^- + HNO$ (≤0.05%)	−243

Heats of reactions are calculated using values in the NIST Webbook unless otherwise noted [10].

[a] Experimental value of SF_4 electron affinity of 1.5 ± 0.2 eV [21].

[b] G3 value of SF_4 electron affinity of 1.64 eV [26].

[c] Relies on heat of formation from Bopp et al. [29].

NH_2^- would be difficult to distinguish, provided the large corrections necessary to account for the $O_2(X)$ reactivity. The efficiency of the charge transfer channel, i.e., the measured rate constant is basically equal to the Langevin collision rate constant, is consistent with the results presented above. This is consistent with other types of energy driving the endothermic charge transfer channel for the reaction of ground electronic state O_2 with NH_2^-.

The reaction of SO_2^- with $O_2(a\ ^1\Delta_g)$ occurs at 20% of the collisional rate constant value. Two main products are observed in about equal abundance, charge transfer and electron detachment. The former has been qualitatively observed by Grabowski et al. [12] in a study of the electron affinity of SO_2. In addition, a small clustering channel to create SO_4^- has been observed in the SIFT, accounting for ~2% of the product ions. The charge transfer reaction is exothermic by 23 kJ mol^{-1}. The reaction efficiency (the experimental rate constant is about 10% of the Langevin value) implies that reasonable coupling with the electronic energy in $O_2(a\ ^1\Delta_g)$ occurs, driving the reactivity. The electron detachment channel is endothermic by 7 kJ mol^{-1} if SO_2 and O_2 products are formed, which may account for the rate constant being smaller than collisional. This production of electrons is a second example of Penning detachment [1], the first example being the reaction of O_2^- with $O_2(a\ ^1\Delta_g)$ discussed in Section 1.

The reaction of CH_3O^- with $O_2(a\ ^1\Delta_g)$ proceeds by hydride transfer both with and without electron detachment. The two product channels are observed in approximately equal abundance. Bierbaum and co-workers have studied this reaction qualitatively in a FA and have observed the HO_2^- product [13,14]. The detachment channel would be difficult to attribute to the $O_2(a)$ reaction because they used microwave discharge generation of $O_2(a)$ without any filtering [13,14], which is known to produce O atoms and O_3 [2]. As shown earlier, the $O_2(X)$ reaction with CH_3O^- also makes both product channels. However, the rate constant for $O_2(X)$ is over 600 times smaller than the $O_2(a\ ^1\Delta_g)$ value, even though both reactions are considerably exothermic. In this case, the electron detachment channel cannot be considered Penning detachment because the reaction also involves a hydrogen transfer.

Three products are formed in the reaction of HO_2^- with $O_2(a\ ^1\Delta_g)$. The main product channel (58%) is Penning detachment and it is essentially thermoneutral. The next most abundant product is charge transfer, which occurs in 29% of reactions. As seen with NH_2^- and SO_2^-, this pathway also requires the electronic energy in $O_2(a\ ^1\Delta_g)$ to drive that channel. Finally, a chemical reaction channel produces O_3^- in 13% of reactions. Bierbaum and co-workers have also studied this reaction in a FA and again qualitatively observed the O_2^- and O_3^- product ions [13,14]. Their experiment would not be able to easily measure the detachment channel contribution for the reasons just discussed. The overall rate constant measured in the SIFT is almost half of the collisional value.

5. Conclusions

We have presented a variety of negative ion–molecule chemistry involving $O_2(a\ ^1\Delta_g)$. Our production method of $O_2(a\ ^1\Delta_g)$ requires a knowledge of the $O_2(X\ ^3\Sigma_g^-)$ reactivity as well and where appropriate this chemistry has been measured. Most of the ions included in this survey are either known not to react with $O_2(X\ ^3\Sigma_g^-)$ [6,20,21] or have been found in the current study not to react, giving upper limits for the rate constants of 1×10^{-12} cm^3 s^{-1}. In contrast, CH_3O^- and NH_2^- do react with $O_2(X)$. The CH_3O^- reaction is very slow (~10^{-12} cm^3 s^{-1}) and proceeds by hydride transfer, both with and without subsequent electron detachment. This reaction is slow enough not to hinder the $O_2(a\ ^1\Delta_g)$ study. The NH_2^- reaction has previously been found to produce OH^- at 300 K in a flowing afterglow. Our room temperature rate constant is about half of the literature value [28]. In addition, we have seen a minor contribution at 300 K from an endothermic charge transfer reaction. Temperature dependences measured for this reaction show that both the branching ratio and individual rate constant for the exothermic channel generating OH^- decreases with increasing temperature, with a concomitant increase in the branching ratio and rate constant for the charge transfer channel up to 700 K.

One of the goals of this study has been to find ion–molecule reactions for which either charge transfer or Penning detachment are driven by the electronic energy in $O_2(a\ ^1\Delta_g)$, i.e., the reactions are endothermic for $O_2(X\ ^3\Sigma_g^-)$. These mechanisms have been observed in our previous studies of the O_2^- reaction with $O_2(a\ ^1\Delta_g)$ [2,3]. Additional reactions have been found to occur by these mechanisms in the present study. In both the HO_2^- and SO_2^- reactions, the charge exchange and Penning detachment channels compete with each other. Penning detachment is very slightly endothermic in both cases and the results show roughly the same reactivity for the two ions. The presence of the charge transfer channel implies that the reaction may proceed in two steps. First, the charge transfer occurs. Then, the excited state ion formed can detach an electron. The division of products between the two channels would be determined by the energy distribution resulting from the charge transfer step. Besides these two reactions, NH_2^- also charge transfers rapidly with $O_2(a\ ^1\Delta_g)$, as opposed to essentially no charge transfer observed with $O_2(X)$. These reactions show that $O_2(a\ ^1\Delta_g)$ can be converted into O_2^- fairly readily, i.e., the electronic energy couples efficiently into the reactivity.

Contrast these observations to the SF_4^- and SF_6^- reactions, where the electronic energy is found not to drive the reactivity. For SF_6^-, this is most likely a result of the geometry difference between the anion and the neutral. The inefficiency of the charge transfer reaction for SF_4^- indicates that the calculated EA of SF_4 is better than the experimental one; although, the differences are within their mutual uncertainties. In addition, the electronic excitation does not appear to be efficient in driving the oxidation mechanism because SO_3^- and CO_3^- have been found to react with $O_2(a)$ at <10^{-11} cm^3 s^{-1}. These may well be due to barriers resulting from splitting the strong O_2 bond.

Acknowledgements

We dedicate this paper to Zdeněk Herman, an esteemed colleague of many years. We would like to acknowledge Bill McDermott, Terry Rawlins, and Steve Davis who provided numerous helpful suggestions on how to work with $O_2(a\ ^1\Delta_g)$. This work was supported by the United States Air Force Office of Scientific Research (AFOSR) under Project No. 2303EP4. AJM was supported through Boston College under Contract No. FA8718-04-C-0006. ID was supported under a National Research Council Research Associateship Award at AFRL.

References

[1] R.S. Berry, Phys. Chem. Chem. Phys. 7 (2005) 289.
[2] A.J. Midey, I. Dotan, S. Lee, W.T. Rawlins, M.A. Johnson, A.A. Viggiano, J. Phys. Chem. A 111 (2007) 5218.
[3] A.J. Midey, I. Dotan, A.A. Viggiano, J. Phys. Chem. A 112 (2008) 3040.
[4] W.T. Rawlins, S. Lee, W.J. Kessler, S.J. Davis, Appl. Phys. Lett. 86 (2005) 051105.
[5] J.C. Poutsma, A.J. Midey, A.A. Viggiano, J. Chem. Phys. 124 (2006) 074301.
[6] S. Williams, M.F. Campos, A.J. Midey, S.T. Arnold, R.A. Morris, A.A. Viggiano, J. Phys. Chem. A 106 (2002) 997.
[7] E.E. Ferguson, J. Phys. Chem. 90 (1986) 731.
[8] F.C. Fehsenfeld, D.L. Albrittion, J.A. Burt, H.I. Schiff, Can. J. Chem. 47 (1969) 1793.
[9] B.L. Upschulte, P.J. Marinelli, B.D. Green, J. Phys. Chem. 98 (1994) 837.
[10] P.J. Linstrom, W.G. Mallard, NIST Chemistry WebBook, NIST Standard Reference Database No. 69, National Institutes of Standards and Technology, Gaithersburg, MD, 2007.

[11] I. Dotan, S.E. Barlow, E.E. Ferguson, Chem. Phys. Lett. 121 (1985) 38.
[12] J.J. Grabowski, J.M. Van Doren, C.H. DePuy, V.M. Bierbaum, J. Chem. Phys. 80 (1984) 575.
[13] R.J. Schmitt, V.M. Bierbaum, C.H. DePuy, J. Am. Chem. Soc. 101 (1979) 6443.
[14] V.M. Bierbaum, R.J. Schmitt, C.H. DePuy, Environ. Health Perspect. 36 (1980) 119.
[15] A.A. Viggiano, R.A. Morris, F. Dale, J.F. Paulson, K. Giles, D. Smith, T. Su, J. Chem. Phys. 93 (1990) 1149.
[16] A.A. Khan, M. Kasha, J. Chem. Phys. 39 (1963) 2105.
[17] H. Seliger, Anal. Biochem. 1 (1960) 60.
[18] W.E. McDermott, N.R. Pchelkin, D.J. Benard, R.R. Bousek, Appl. Phys. Lett. 32 (1978) 469.
[19] Y. Ikezoe, S. Matsuoka, M. Takebe, A.A. Viggiano, Gas Phase Ion-Molecule Reaction Rate Constants Through 1986, Maruzen Company, Ltd., Tokyo, 1987.
[20] A.A. Viggiano, S.T. Arnold, S. Williams, T.M. Miller, Plasma Chem. Plasma Proc. 22 (2002) 285.
[21] A.E.S. Miller, T.M. Miller, A.A. Viggiano, R.A. Morris, J.M.V. Doren, S.T. Arnold, J.F. Paulson, J. Chem. Phys. 102 (1995) 8865.
[22] G.E. Streit, J. Phys. Chem. 86 (1982) 2321.
[23] S. Chowdhury, P. Kebarle, J. Chem. Phys. 85 (1986) 4989.
[24] E.P. Grimsrud, S. Chowdhury, P. Kebarle, J. Chem. Phys. 83 (1985) 1059.
[25] J.C. Bopp, J.R. Roscioli, M.A. Johnson, T.M. Miller, A.A. Viggiano, S.M. Villano, S.W. Wren, W.C. Lineberger, J. Chem. Phys. 111 (2007) 1214.
[26] T.M. Miller, S.T. Arnold, A.A. Viggiano, Int. J. Mass Spectrom. 227 (2003) 413.
[27] A.A. Viggiano, T.M. Miller, J.F. Friedman, J. Troe, J. Chem. Phys. 127 (2007) 244305.
[28] G.E. Streit, J. Chem. Phys. 77 (1982) 826.
[29] J.C. Bopp, J.M. Headrick, J.R. Roscioli, M.A. Johnson, A.J. Midey, A.A. Viggiano, J. Chem. Phys. 124 (2006) 174302.